

Supporting Information for

A novel 3-D thioindate-thioantimonate based on the linkages of large heterometallic $\{\text{In}_2\text{Sb}_2\text{S}_9\}$ clusters and 1-D $[\text{In}_2\text{Sb}_2\text{S}_8]_n^{4-}$ chains

Jian Zhou, and Litao An

Table S1. Selected Bond Lengths (\AA) and Angles (deg) for **1.**

In(1)-S(3)	2.4299(15)	In(2)-S(5)	2.4173(17)
In(1)-S(5)	2.4310(18)	In(2)-S(6)	2.4500(17)
In(1)-S(2)	2.4539(18)	In(2)-S(10)#1	2.4828(17)
In(1)-S(4)	2.4630(18)	In(2)-S(11)	2.4901(17)
In(3)-S(7)#2	2.4329(17)	Sb(1A)-S(2)	2.433(2)
In(3)-S(1)#2	2.4513(18)	Sb(1A)-S(1)	2.436(2)
In(3)-S(9)	2.4637(18)	Sb(1A)-S(4)#3	2.454(2)
In(3)-S(8)	2.4652(19)	Sb(2)-S(6)	2.4255(17)
Sb(3)-S(10)	2.4166(17)	Sb(2)-S(7)	2.4542(18)
Sb(3)-S(11)	2.4218(16)	Sb(2)-S(8)	2.4613(17)
Sb(3)-S(9)	2.4233(17)	Co(2)-N(7)	2.141(19)
Co(1)-N(1)	2.150(7)	Co(2)-N(11)	2.153(15)
Co(1)-N(6)	2.158(7)	Co(2)-N(10)	2.17(3)
Co(1)-N(5)	2.168(6)	Co(2)-N(9)	2.171(18)
Co(1)-N(4)	2.176(7)	Co(2)-N(8)	2.188(19)
Co(1)-N(3)	2.180(7)	Co(2)-N(12)	2.192(15)
Co(1)-N(2)	2.197(6)	S(3)-In(1)-S(5)	109.28(7)
S(5)-In(2)-S(6)	124.28(6)	S(3)-In(1)-S(2)	112.50(5)
S(5)-In(2)-S(10)#1	101.84(6)	S(5)-In(1)-S(2)	107.56(7)
S(6)-In(2)-S(10)#1	104.30(6)	S(3)-In(1)-S(4)	107.28(5)
S(5)-In(2)-S(11)	113.13(7)	S(5)-In(1)-S(4)	110.43(7)
S(6)-In(2)-S(11)	102.25(6)	S(2)-In(1)-S(4)	109.81(7)
S(10)#1-In(2)-S(11)	110.49(6)	S(7)#2-In(3)-S(1)#2	111.21(7)
S(2)-Sb(1A)-S(1)	95.45(9)	S(7)#2-In(3)-S(9)	103.06(6)
S(2)-Sb(1A)-S(4)#3	101.09(8)	S(1)#2-In(3)-S(9)	110.74(8)
S(1)-Sb(1A)-S(4)#3	90.70(7)	S(7)#2-In(3)-S(8)	111.07(7)
S(6)-Sb(2)-S(7)	90.55(6)	S(1)#2-In(3)-S(8)	106.07(7)
S(6)-Sb(2)-S(8)	95.91(6)	S(9)-In(3)-S(8)	114.80(6)
S(7)-Sb(2)-S(8)	95.47(7)	S(10)-Sb(3)-S(11)	92.77(6)
N(1)-Co(1)-N(6)	95.7(3)	S(10)-Sb(3)-S(9)	99.14(6)
N(1)-Co(1)-N(5)	169.5(3)	S(11)-Sb(3)-S(9)	98.49(6)

N(6)-Co(1)-N(5)	80.0(3)	N(7)-Co(2)-N(11)	92.7(7)
N(1)-Co(1)-N(4)	93.0(3)	N(12) ^{#3} -Co(2)-N(10)	31.6(8)
N(6)-Co(1)-N(4)	168.6(3)	N(7)-Co(2)-N(10)	94.4(8)
N(5)-Co(1)-N(4)	92.6(3)	N(11)-Co(2)-N(10)	168.2(8)
N(1)-Co(1)-N(3)	92.3(3)	N(7)-Co(2)-N(9)	170.9(7)
N(6)-Co(1)-N(3)	92.6(3)	N(11)-Co(2)-N(9)	93.5(7)
N(5)-Co(1)-N(3)	97.4(3)	N(10)-Co(2)-N(9)	80.7(7)
N(4)-Co(1)-N(3)	79.8(3)	N(7)-Co(2)-N(8)	79.1(6)
N(1)-Co(1)-N(2)	79.0(3)	N(11)-Co(2)-N(8)	95.4(6)
N(6)-Co(1)-N(2)	90.7(3)	N(10)-Co(2)-N(8)	95.2(8)
N(5)-Co(1)-N(2)	91.4(2)	N(9)-Co(2)-N(8)	93.7(6)
N(4)-Co(1)-N(2)	98.2(3)	N(7)-Co(2)-N(12)	95.7(7)
N(3)-Co(1)-N(2)	171.0(3)	N(11)-Co(2)-N(12)	78.9(5)
N(9)-Co(2)-N(12)	92.0(7)	N(10)-Co(2)-N(12)	90.9(8)
N(8)-Co(2)-N(12)	172.2(7)		

Symmetry transformations used to generate equivalent atoms: (#1) $-x+1, -y, -z+1$; (#2) $-x+3/2, -y+1/2, -z+1$; (#3) $-x+1, y, -z+1/2$.

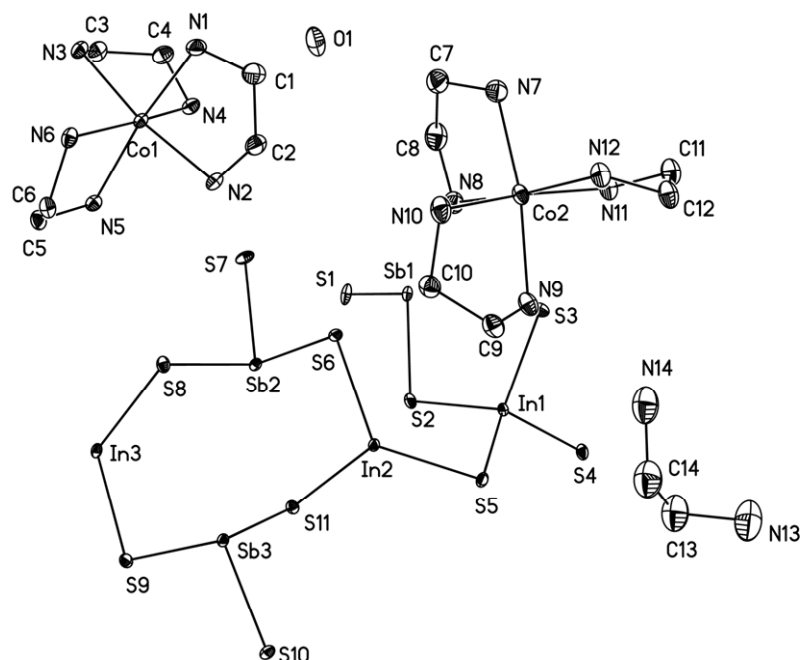


Figure S1 The asymmetric unit of **1** with labeling scheme and 30% probability ellipsoids. H atoms are omitted for clarity.

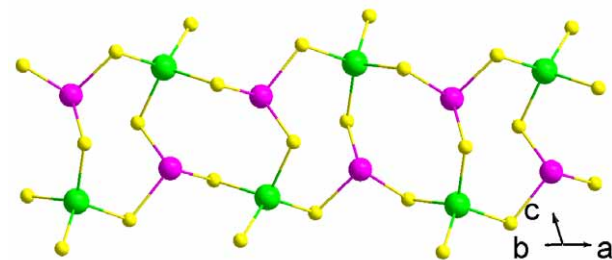


Figure S2 1-D $[\text{In}_2\text{Sb}_2\text{S}_8^{4-}]_n$ chain along the [110] direction.

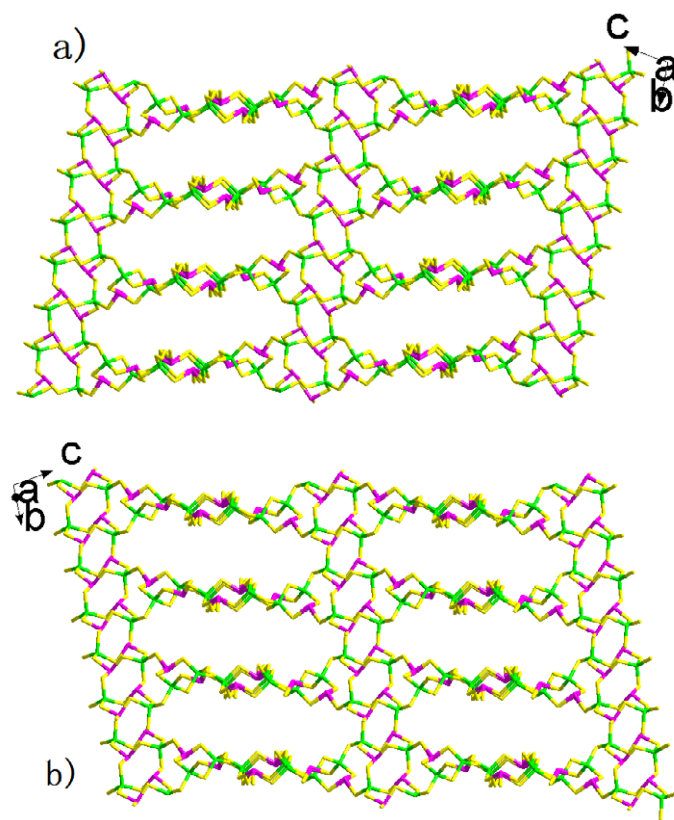


Figure S3 View of the 3D framework in 1 showing 20-ring channels along the [-110](a) and [1-10] (b) directions.

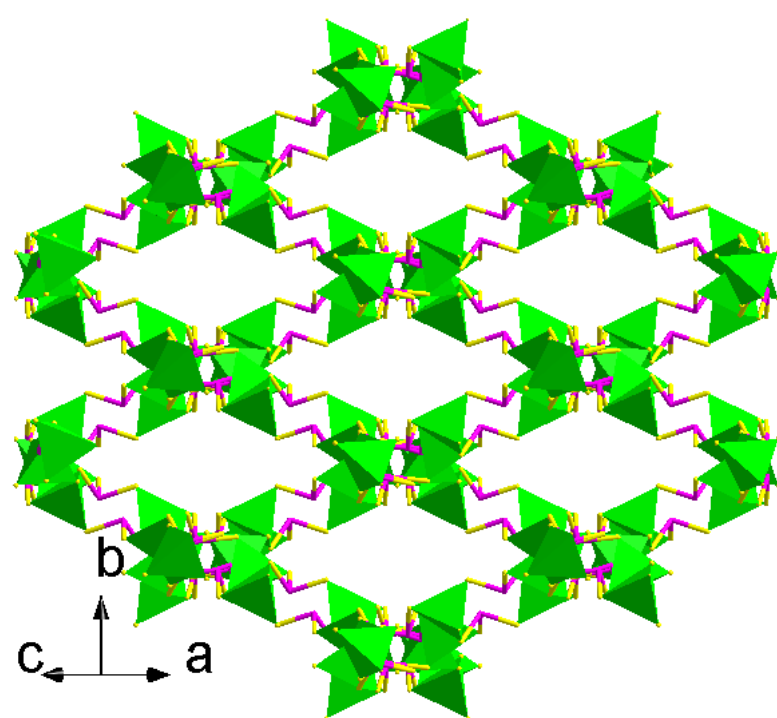


Figure S4 View of the 3D framework in **1** showing 14-ring channels along the [101] direction.

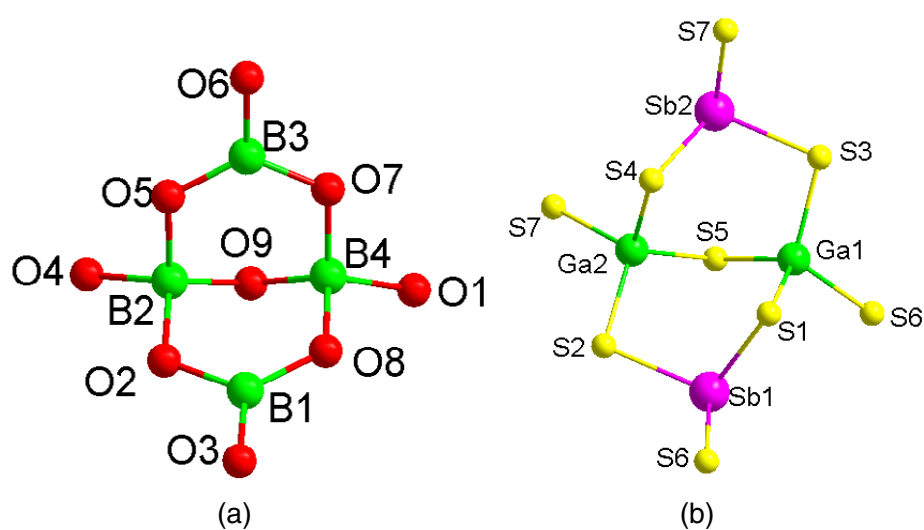


Figure S5 The structures of $[B_4O_9]$ (a) and $[Ga_2Sb_2S_9]$ (b) clusters.

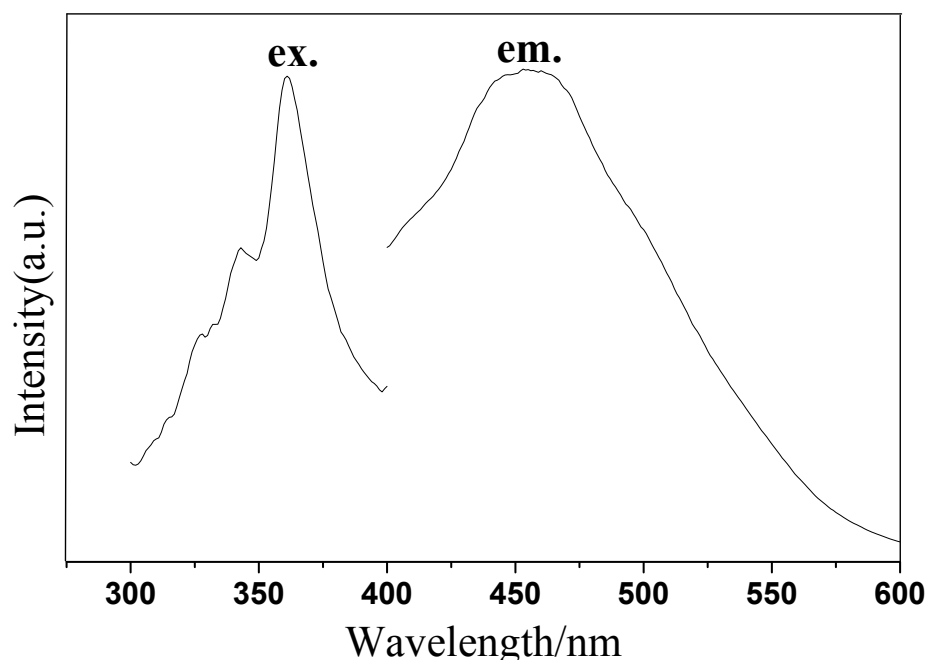


Figure S6 The solid-state excitation and emission spectra of **1** at room temperature.

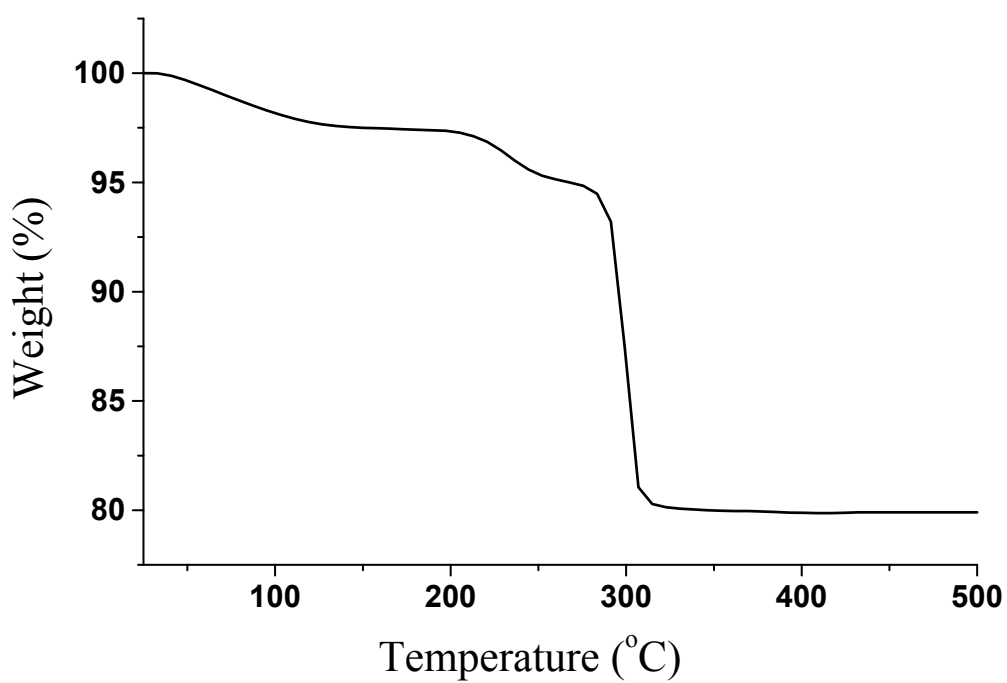


Figure S7. TG curve of **1**.

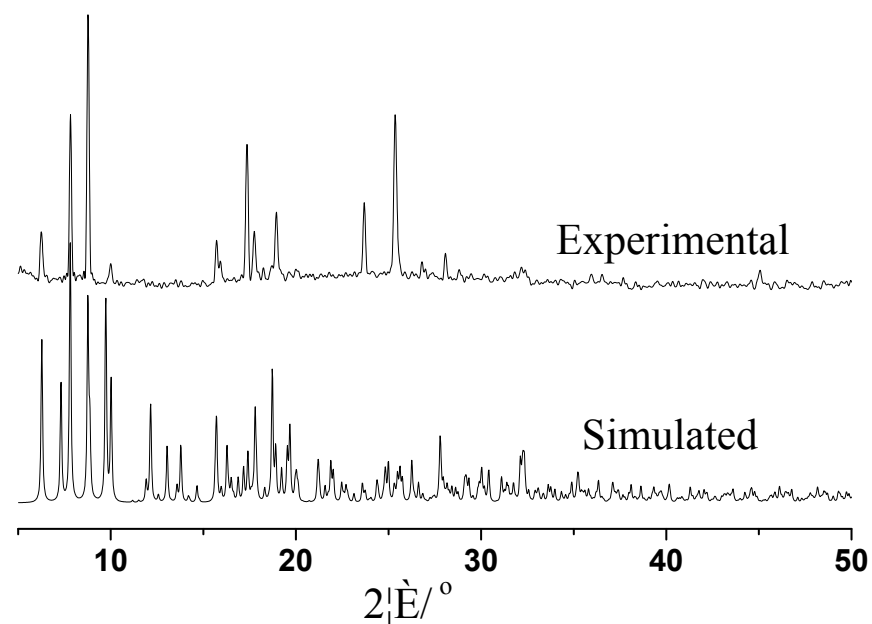


Figure S8. The XRD result of **1**.

The experimental peak positions are in agreement with simulated XRD pattern, indicating the phase purity of 1. The difference in reflection intensity between experimental and simulated XRD patterns is probably due to the preferred orientation effect of the powder sample during collection of the experimental XRD data.

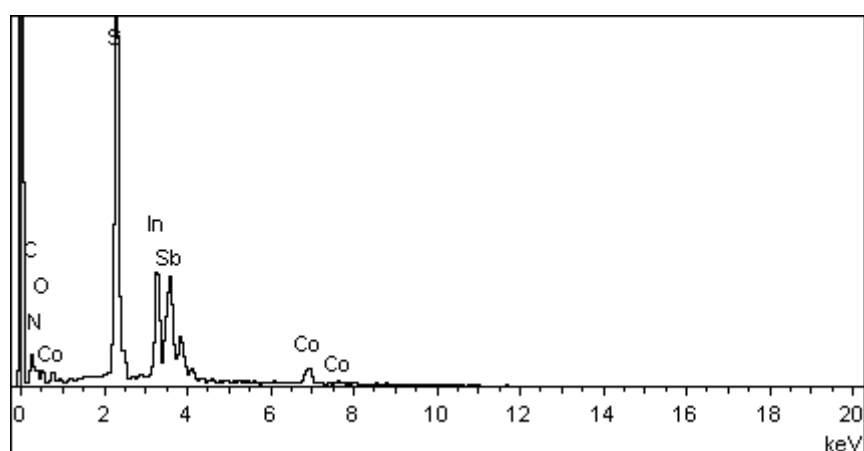


Figure S9. EDS spectrum of **1**.

The energy dispersive spectroscopy (EDS) analyses show that molar ratio of In:Sb:Co:S is 2.10:1.96:1.08:6.98, which is very close to the stoichiometry.